

Ab Initio and Density Functional Theory Study of the Geometric Structure, Vibrational Frequency, Torsional Potential, and Isomerization of Dichlorodisulfane (CISSCI)

Debananda Das[†] and Scott L. Whittenburg*

Department of Chemistry, University of New Orleans, New Orleans, Louisiana 70148

Received: October 23, 1998; In Final Form: January 19, 1999

The equilibrium geometric structure and vibrational frequency of CISSCI have been determined at HF, MP2, LSDA, BLYP, B3LYP, BP86, B3P86, and B3PW91 level using different basis sets with diffuse and d and f polarization functions. Comparison with available experimental and theoretical results have been made. The effect of basis set on the accuracy of the prediction of dipole moment has been examined. The effect of internal rotation on the structural parameters has been analyzed, and torsional potentials at ab initio and density functional levels have been determined. Analysis of the relative stability of CISSCI with respect to SSCl₂ using hybrid density functionals at 6-311+G(3df) basis set indicates that the former is more stable by 10–12 kcal mol⁻¹. The activation energy for the isomerization of CISSCI to SSCl₂ has been determined, using the correlated methods, to be between 40 and 48 kcal mol⁻¹.

Introduction

The chemistry of sulfur compounds has been an area of active research over the years. Small sulfur-containing molecules have many industrial applications. The S–S linkage is of great importance in many biologically important glycoproteins. One such glycoprotein is fibronectin which plays a crucial role in such diverse processes as cell adhesion, cell migration, cell differentiation, oncogenic transformation, and maintenance of normal cell morphology. Sulfur-containing molecules such as dimethyl sulfide, dimethyl disulfide, disulfane (H₂S₂), difluorodisulfane (S₂F₂), and dichlorodisulfane (S₂Cl₂) exhibit large-amplitude motion¹ and are of fundamental importance.

S₂Cl₂ is one of the simpler disulfides characterized by an unusually short S–S bond. The sulfur–sulfur and sulfur–halogen bond distance is difficult to reproduce accurately by theoretical calculations.² Accurate reproduction of the geometry by theoretical models can help benchmark calculations for molecules of the same class. We have examined the equilibrium geometric structure, vibrational frequency, torsional potential function, and isomerization of S₂Cl₂.

Computational Methodology

Over the past few years, density functional theory^{3,4} has become an attractive choice for electronic structure calculations. Its accuracy is comparable to high-level ab initio methods without being as expensive in terms of computer resources. Standard ab initio molecular orbital calculations⁵ and density functional theory calculations on CISSCI and SSCl₂ were performed using GAUSSIAN 94.⁶ The default GAUSSIAN convergence criteria⁷ was used for all geometry optimizations. While determining the equilibrium geometry, the nature of the stationary point was further confirmed by the absence of any imaginary frequency.

For the ab initio calculations, Hartree–Fock (HF) self-consistent field (SCF) and second-order Møller–Plesset⁸ (MP2) perturbation theory were used. Quadratic configuration interaction⁹ including single and double substitutions (QCISD) were

performed to understand the effect of higher order electron correlation on geometry, cis–trans rotational barriers, and energetics of the isomerization reaction. For density functional calculations, hybrid density functionals^{10,11} were used since they yield much better results. Becke's three-parameter exchange function¹¹ (B3) was used along with three different sets of correlation functionals. They are the functionals due to Lee, Yang, and Parr (LYP),¹² the functionals due to Perdew,^{13,14} (P86) and the functionals due to Perdew and Wang¹⁵ (PW91). The exchange and correlation functionals taken together are commonly represented as B3LYP, B3P86, and B3PW91. In some cases, computations utilizing local spin density approximation^{16,17} (LSDA functional) and the gradient corrected BLYP and BP86 functionals^{12–14,18} have been performed to analyze their performance vis-à-vis the hybrid functionals. For CISSCI, the effect on equilibrium geometry of systematic increase in the size of basis set along with the addition of diffuse functions as well as d and f polarization functions have been analyzed by using 6-31G(d), 6-311G(d), 6-311+G(d), 6-311G(2d), 6-311G(df), 6-311+G(2df), and 6-311+G(3df) basis sets.¹⁹ For SSCl₂, the equilibrium geometry has been determined at HF, B3LYP, B3P86, and B3PW91 functionals using the 6-311+G(3df) basis set. The MP2 geometry for this molecule has been determined at 6-311+G(2df) basis.

For locating the transition state for the CISSCI to SSCl₂ isomerization, the synchronous transit-guided quasi-newton (STQN) method of Schlegel and co-workers²⁰ has been implemented. The stationary point for the transition state is further characterized by the presence of one imaginary frequency.

In this work, the torsional potential function of S₂Cl₂ at the 6-311+G(3df) basis set using HF, MP2, B3LYP, B3P86, and B3PW91 has been examined. The effect of torsion on the S–S and S–Cl bond lengths, as well as on the S–S–Cl bond angle, has been studied. The energy barriers to cis ($\tau = 0$) and trans ($\tau = 180$) torsions at several ab initio and density functional levels have been determined.

Structure of S₂Cl₂

The equilibrium geometric structure of CISSCI has been studied. Cárdenas-Jirón and co-workers²¹ reported the equilib-

* Corresponding author. E-mail: swhitten@uno.edu.

[†] E-mail: das_deb@hotmail.com.

rium structure at the HF-SCF level using a 6-31G basis including polarization and diffuse orbitals over all the atoms in the molecule. The deviation from an early electron diffraction structure of Hirota²² is nearly 2%. It predicts a S-S bond distance slightly more than 2.0 Å. The Cl-S-S-Cl dihedral (τ) of nearly 95° appears very high. Samdal and co-workers²³ have also calculated the equilibrium structure at the HF/6-31G(d) level. Besides predicting a S-S bond distance slightly greater than 2.0 Å, it underestimates the S-S-Cl bond angle by about 2°. However, the dihedral angle has been predicted well. Schleyer and co-workers²⁴ have studied the equilibrium structure at the HF/6-31G(d), MP2/6-31G(d), and MP2/6-311G(2d) levels. Their MP2 calculations predict a S-S bond distance slightly less than 2.0 Å. Altmann, Handy, and Ingamells²⁵ had evaluated the performance of numerical basis sets vis-à-vis Gaussian basis sets for a variety of sulfur-containing molecules. They used three sets of density functionals, namely, the local density approximation^{17,26} (LDA), BVWN, which comprises Becke's exchange¹⁸ correction (B) and the Vosko, Wilk, Nusair (VWN) correlation function,¹⁷ and BLYP in which the correlation functional is due to Lee, Yang, and Parr.¹² The geometry of S₂Cl₂ was poorly predicted in this study. In a subsequent paper,²⁷ Altmann, Handy, and Ingamells predicted the structure using B3P86, MP2, and HF theory using 6-31G(d) and Dunning's correlation consistent triple- ζ set²⁸ with built in polarization functions (cc-pVTZ). There is substantial improvement in the prediction of the equilibrium geometry using the B3P86 hybrid exchange correlation functional, and the results are comparable to those of MP2 at the same basis set. These studies indicate the difficulty in computing the S-S and S-Cl bond lengths.

Our results with the addition of f polarization functions and diffuse functions improve the accuracy of the equilibrium bond distance. There is not a substantial improvement in bond angles. The performance of B3P86 at 6-311+G(3df) has not been previously studied. Also, the performance of the hybrid B3LYP and B3PW91 functionals has been evaluated. The effect of basis sets of enlarged sizes with diffuse functions and d and f polarization functions is analyzed.

The calculated structural parameters for S₂Cl₂ are given in Table 1. The experimental microwave (MW) and electron diffraction (ED) data have also been given for comparison.^{29,30} The former has uncertainties related to zero-point vibrations, while the later has uncertainties due to electron correlation. Besides having different numbers of significant figures, there is a difference of about 0.02 Å in the S-S bond length between the two experimental data. Still both indicate a S-S bond distance shorter by about 0.1 Å than the typical S-S single bond length³¹ of about 2.05 Å. HF predicts a S-S bond length slightly longer than 2 Å at 6-31G(d), 6-311G(d), 6-311+G(d), and 6-311G(df) basis sets. The inclusion of higher polarization functions shortens the S-S bond length below 2 Å. At 6-311+G(3df) basis set, HF overestimates the S-S bond length by 0.0295 Å from the microwave data and by 0.049 Å from the electron diffraction data. HF is known to underestimate bond lengths, but for S₂Cl₂, it overestimates the S-S bond length at all basis sets. MP2, B3LYP, B3P86, and B3PW91 all predict a S-S bond length less than 2 Å at all basis sets studied. In general, the S-S bond shortens with incremental treatment of diffuse and d and f polarization functions. MP2 at 6-311+G(3df) differs from the microwave (MW) by 0.004 Å and from the electron diffraction (ED) data by 0.015 Å. At the 6-311+G(2df) level, the S-S bond length at MP2 theory differs from microwave by 0.009 Å and from electron diffraction by 0.028 Å. The differences between the microwave data and those due

to B3LYP, B3P86, and B3PW91 at 6-311+G(3df) are 0.0014, 0.013, and 0.0107 Å, respectively (all underestimates). The differences from the electron diffraction data for the above three density functionals are 0.018, 0.006, and 0.009 Å, respectively (all overestimates).

At 6-311+G(3df), HF underestimates the S-Cl bond length by 0.0245 Å from the microwave data and by 0.026 Å from the ED data. The differences for MP2 are 0.0031 Å from MW and 0.005 Å from ED. The density functionals overestimate the S-Cl bond length at all basis sets.

HF underestimates the S-S-Cl bond angle by about 2° at all basis sets, while all three density functionals overestimate it by about the same amount. All three hybrid density functionals predict essentially the same Cl-S-S bond angle and dihedral. The local (LSDA) and gradient corrected functionals (BLYP and BP86) show the largest deviation in S-S-Cl bond angle. MP2 shows the best agreement among all theoretical models to the experimental bond angle. The traditional ab initio methods, HF and MP2, reproduce the Cl-S-S-Cl dihedral excellently. Almost all the values are within the standard deviation of the experimental values. The density functionals reproduce the dihedral as well as the ab initio methods. Diffuse functions as well as increased complexity of d and f polarization functions do not change the accuracy of bond angle and Cl-S-S-Cl dihedral prediction for a given theoretical method. The largest effect of enlarged basis sets is on the S-S and S-Cl bond lengths. Overall, the 6-311+G(2df) and 6-311+G(3df) basis sets produce excellent agreement. MP2 produces the closest agreement with the experimental geometries. QCISD/6-311G(d), despite being much more computationally demanding, does not show any significant improvement over MP2 at the same basis. All density functionals do reasonably well in the prediction of bond lengths with B3P86 showing the closest agreement.

As expected, the highest basis set 6-311+G(3df) produces the lowest energy for a given theoretical model.³² The relative order of energies predicted for a given basis set are LSDA > HF > MP2 > QCISD > B3PW91 > BLYP > B3LYP > BP86 > B3P86, with the difference between LSDA and B3P86 being about 6 hartrees.³³

Vibrational Frequency

The vibrational frequency of S₂Cl₂ has been determined. At the MP2 level, the calculation has been done at the 6-311G(d) basis set. Besides 6-311G(d), the 6-311+G(3df) basis set has been used for HF, B3LYP, B3P86, and B3PW91 to understand the effect of diffuse and d and f polarization functions. Frequencies at local (LSDA) and gradient corrected levels have also been computed for comparison with the hybrid functionals. All derivatives have been calculated analytically. The calculated frequencies have not been scaled. The scaling factors reported in the literature are dependent not only on the method used but also on the basis set.³⁴ Moreover, the accuracy of the scaling factor depends on the types of molecules used in the benchmark. The available scaling factors might not be appropriate for the present study.

The calculated vibrational frequency along with the best available experimental³⁵ fundamental vibrations have been reported in Table 2. The computed intensities have been given in parentheses. The calculated and experimental frequencies match extremely well. Some vibrations at the HF level are grossly overestimated though. Examination of root-mean-square (RMS) deviation of the calculated frequencies reveals that inclusion of diffuse and three sets of d and f polarization function

TABLE 1: Cl–S–S–Cl Bond Length and Bond Angles

		$r(\text{S–S}) \text{ \AA}$	$r(\text{Cl–S}) \text{ \AA}$	$\alpha(\text{Cl–S–S})^\circ$	$\tau(\text{Cl–S–S–Cl})^\circ$	
expt ²⁹		1.9504(12)	2.0552(7)	107.66(5)	85.24(10)	
expt ³⁰		1.931(5)	2.057(2)	108.2(0.3)	85.8(1.3)	
HF	6-31G(d)	2.0033	2.0400	105.9	85.0	
	6-311G(d)	2.0092	2.0538	105.6	85.0	
	6-311+G(d)	2.0119	2.0517	105.6	85.2	
	6-311G(2d)	1.9987	2.0546	105.8	85.2	
	6-311G(df)	2.0031	2.0416	105.9	84.7	
	6-311+G(2df)	1.9874	2.0366	106.0	85.2	
	6-311+G(3df)	1.9799	2.0307	106.2	85.1	
	MP2	6-31G(d)	1.9809	2.0721	107.5	85.8
		6-311G(d)	1.9767	2.0900	107.4	85.8
		6-311+G(d)	1.9811	2.0853	107.2	85.3
6-311G(2d)		1.9753	2.0976	107.5	85.7	
6-311G(df)		1.9637	2.0477	107.8	85.3	
6-311+G(2df)		1.9594	2.0601	107.2	85.2	
6-311+G(3df)		1.9464	2.0521	107.5	85.1	
QCISD	6-31G(d)	1.9981	2.0802	106.7	85.7	
	6-311G(d)	2.0001	2.0944	106.6	85.7	
B3LYP	6-31G(d)	1.9819	2.1215	109.4	87.1	
	6-311G(d)	1.9757	2.1441	109.2	87.1	
	6-311+G(d)	1.9789	2.1386	109.2	87.3	
	6-311G(2d)	1.9646	2.1238	109.1	87.2	
	6-311G(df)	1.9773	2.1215	109.1	86.9	
	6-311+G(2df)	1.9581	2.1023	109.1	87.0	
	6-311+G(3df)	1.9490	2.0968	109.5	87.1	
	B3P86	6-31G(d)	1.9669	2.0955	109.4	86.9
		6-311G(d)	1.9617	2.1134	109.0	86.9
		6-311+G(d)	1.9649	2.1093	109.1	87.0
6-311G(2d)		1.9506	2.0948	109.0	86.9	
6-311G(df)		1.9631	2.0935	109.1	86.6	
6-311+G(2df)		1.9453	2.0749	108.9	86.8	
6-311+G(3df)		1.9374	2.0692	109.2	86.8	
B3PW91	6-31G(d)	1.9690	2.0980	109.5	87.0	
	6-311G(d)	1.9638	2.1147	109.2	87.0	
	6-311+G(d)	1.9672	2.1108	109.2	87.1	
	6-311G(2d)	1.9524	2.0965	109.2	87.1	
	6-311G(df)	1.9653	2.0953	109.3	86.7	
	6-311+G(2df)	1.9475	2.0768	109.0	86.9	
	6-311+G(3df)	1.9397	2.0718	109.4	86.9	
	BLYP	6-31G(d)	1.9817	2.1852	111.6	88.3
		6-311G(d)	1.9717	2.2164	111.4	88.7
		6-311+G(d)	1.9750	2.2088	111.5	88.6
6-311+G(3df)		1.9495	2.1537	111.4	88.2	
BP86	6-31G(d)	1.9690	2.1517	111.5	88.0	
	6-311G(d)	1.9609	2.1770	111.1	88.2	
	6-311+G(d)	1.9635	2.1695	111.3	88.1	
	6-311+G(3df)	1.9404	2.1175	111.0	87.7	
LSDA	6-31G(d)	1.9469	2.1040	111.1	87.1	
	6-311G(d)	1.9370	2.1268	110.6	87.2	
	6-311+G(3df)	1.9176	2.0698	110.2	86.6	

decreases the RMS deviation by a factor of 2 for the hybrid density functionals. HF is not as accurate as the higher level correlated methods. The density functionals produce excellent agreement with B3P86 and B3PW91 producing lower RMS deviation than B3LYP. The hybrid functionals also produce lower RMS deviation than the gradient corrected functionals. Surprisingly, LSDA frequencies are comparable to the hybrid results. MP2 produces the best agreement of all calculated frequencies and its RMS deviation at 6-311G(d) basis set is comparable to those of B3P86 and B3PW91 at 6-311+G(3df).

Dipole Moment

The calculated dipole moments of S_2Cl_2 at HF, MP2, B3LYP, B3P86, and B3PW91 at different basis sets have been given in Table 3. BLYP and BP86 dipole moments at selected basis sets have also been given. There is a wide variation in the value in going from 6-31G(d) to 6-311+G(3df) basis set. The authors are not aware of any experimental value for the dipole moment of S_2Cl_2 . However, analysis of dipole moments³⁶ of selected

sulfides and dimethyl ether show that the dipole moment is very sensitive to the quality of the basis set and is reproduced best at 6-311+G(3df). The experimental³⁷ dipole moments (in debyes) of H_2S_2 (1.17 ± 0.02), S_2F_2 (1.45 ± 0.02), dimethyl sulfide (1.554), and dimethyl ether (1.30) match extremely well with the B3LYP/6-311+G(3df) calculated values of 1.12, 1.58, 1.59, and 1.29 D and B3P86/6-311+G(3df) values of 1.15, 1.44, 1.61, and 1.26 D, respectively. HF and MP2 do not predict dipole moments as accurately as the hybrid density functionals for these molecules.³⁸ A closer examination reveals that the dipole moment predicted using B3P86 functional is almost identical with the experimental dipole moments³⁷ of HSSH and FSSF. The dipole moment calculated at B3P86/6-311+G(3df) for the analogous ClSSCl might be more representative of the actual value.

Torsion

The torsional potential of dichlorodisulfane (S_2Cl_2) has been determined in this work. Koput³⁹ had determined the torsional

TABLE 2: Vibrational Frequency (in cm^{-1}) and Intensity (KM/mol) of S_2Cl_2

	A	A	A	A	B	B	Δ^c
expt ³⁵	95(vvw)	210(vvw)	452(s)	546(w)	244(w)	461(w)	
HF ^a	94(0.5)	213(0.0)	526(8.2)	549(32.1)	264(5.8)	531(71.2)	0.097
HF ^b	96(0.2)	219(0.0)	541(13.5)	564(22.5)	267(4.2)	539(80.0)	0.115
MP2 ^a	97(0.3)	207(0.3)	457(41.7)	517(5.8)	245(8.0)	450(937)	0.026
BLYP ^a	83(0.3)	185(1.8)	348(38.0)	520(15.9)	204(12.2)	335(149.9)	0.177
BLYP ^b	88(0.1)	194(1.1)	385(33.3)	545(11.5)	213(9.4)	368(150.5)	0.123
B3LYP ^a	93(0.4)	198(0.9)	406(45.8)	512(9.4)	227(9.4)	395(133.1)	0.085
B3LYP ^b	95(0.1)	205(0.5)	438(36.4)	545(7.8)	234(6.9)	424(132.1)	0.040
BP86 ^a	87(0.3)	193(1.4)	375(41.4)	538(16.2)	214(11.1)	360(160.6)	0.133
BP86 ^b	91(0.1)	200(0.7)	415(33.9)	565(11.2)	222(7.3)	398(154.3)	0.080
B3P86 ^a	95(0.4)	204(0.6)	432(46.8)	533(10.5)	235(8.7)	419(138.5)	0.047
B3P86 ^b	97(0.1)	210(0.3)	463(35.8)	566(8.1)	240(5.9)	448(132.7)	0.024
B3PW91 ^a	96(0.4)	204(0.6)	431(46.1)	532(10.5)	235(8.7)	418(137.7)	0.048
B3PW91 ^b	97(0.1)	210(0.3)	462(35.3)	564(8.2)	240(5.9)	447(132.2)	0.023
LSDA ^a	91(0.4)	203(0.9)	413(45.0)	571(17.1)	225(9.1)	396(172.6)	0.080
LSDA ^b	93(0.1)	209(0.3)	452(34.8)	597(10.9)	233(5.5)	435(155.2)	0.049

^a 6-311G(d) basis set. ^b 6-311+G(3df) basis set. ^c RMS deviation $\{(1/n_p)\sum((\nu_{\text{calc}} - \nu_{\text{expt}})/\nu_{\text{expt}})^2\}^{1/2}$.

TABLE 3: S_2Cl_2 Dipole Moment (Debye)

basis set	HF	MP2	BLYP	B3LYP	BP86	B3P86	B3PW91
6-31G(d)	1.07	1.21	1.54	1.31	1.39	1.20	1.20
6-311G(d)	1.17	1.34	1.88	1.56	1.70	1.43	1.41
6-311+G(d)	1.10	1.26	1.78	1.48	1.60	1.35	1.33
6-311G(2d)	1.02	1.24		1.32		1.18	1.17
6-311G(df)	1.10	1.12		1.42		1.30	1.28
6-311+G(2df)	0.89	1.02		1.18		1.04	1.03
6-311+G(3df)	0.76	0.88	1.30	1.06	1.10	0.91	0.90

potential energy function for the analogous H_2S_2 . Cárdenas-Jirón and co-workers²¹ had investigated the conformational dependence of various global and local molecular properties using the HF/6-31+G(d) generated potential function of S_2Cl_2 . Samdal and co-workers²³ had examined the effect of Cl-S-S-Cl torsion on the change in S-Cl, S-S bond distances, and S-S-Cl bond angle at HF/6-31G(d). In a previous paper,⁴⁰ they had outlined the importance of such study in the interpretation of electron diffraction data. However, for effective utilization in the interpretation of the electron diffraction data or in the investigation of any property dependent on conformation, it is essential not only to take account of electron correlation but also to have a larger basis set. The results reported here are a vast improvement in that direction.

The structural parameters and relative energy (with respect to the equilibrium energy) have been given in Table 4. The

potential has been determined at the 6-311+G(3df) basis set. The Cl-S-S-Cl dihedral was constrained at 20° intervals from 0° to 180°. Full geometry optimization at the constrained dihedral angle was performed to obtain fully relaxed points on the potential surface. The cis barrier to internal rotation ($\tau = 0$) is higher than the trans barrier ($\tau = 180$) by about 4 kcal mol⁻¹ at all levels of theory. This could be due to the spatial proximity of the two Cl atoms and the ensuing steric repulsion in the cis conformation. The hybrid density functionals predict the cis barrier to be near 22 kcal mol⁻¹. The barrier predicted⁴¹ at the local spin density approximation and nonlocal BLYP and BP86 levels at 6-311+G(3df) basis set is higher by about 2 kcal mol⁻¹. HF and MP2 at the 6-311+G(3df) basis predict barriers of 18.44 and 20.22 kcal mol⁻¹, respectively. QCISD/6-31G(d) predicts a cis barrier of 18.18 kcal mol⁻¹. The hybrid density functionals predict a barrier of nearly 18 kcal mol⁻¹ for the trans rotation. As in the case of the cis barrier, the trans barrier predicted⁴² by LSDA, BLYP, and BP86 is higher than the cis barrier by nearly 2 kcal mol⁻¹. The values predicted by MP2 and HF are nearly 15 and 12 kcal mol⁻¹, respectively. QCISD/6-31G(d) predicts a trans barrier of 14.09 kcal mol⁻¹. There are no experimental data available for the cis and trans barriers of S_2Cl_2 . Hence, analysis of the accuracy of prediction of the cis and trans barriers by different ab initio and density functional methods is not possible.

TABLE 4: Changes in Structural Parameters and Relative Energy (kcal mol⁻¹) as a Function of the Cl-S-S-Cl Torsion Angle for ab Initio and DFT Methods at 6-311+G(3df) Basis Set

torsion		0	20	40	60	80	100	120	140	160	180
B3LYP	S-Cl	2.0191	2.0303	2.0635	2.0865	2.0954	2.0994	2.0967	2.0633	2.0415	2.0383
	S-S	2.1969	2.1437	2.0313	1.9707	1.9517	1.9513	1.9716	2.0553	2.1227	2.1359
	S-S-Cl	105.9	106.3	107.1	108.2	109.2	109.5	108.3	103.0	98.0	96.3
	ΔE	21.95	19.05	11.41	3.95	0.27	0.91	5.75	12.74	16.80	17.74
B3PW91	S-Cl	1.9996	2.0105	2.0410	2.0613	2.0703	2.0721	2.0701	2.0418	2.0217	2.0194
	S-S	2.1726	2.1203	2.0169	1.9607	1.9414	1.9425	1.9645	2.0401	2.1013	2.1136
	S-S-Cl	105.8	106.1	106.9	108.1	109.1	109.4	108.1	102.9	97.8	96.0
	ΔE	22.48	19.43	11.55	3.99	0.26	0.96	5.90	13.02	17.20	18.17
B3P86	S-Cl	1.9977	2.0091	2.0397	2.0598	2.0681	2.0722	2.0690	2.0409	2.0203	2.0172
	S-S	2.1700	2.1174	2.0136	1.9579	1.9394	1.9397	1.9604	2.0357	2.0973	2.1102
	S-S-Cl	105.5	105.9	106.7	107.9	109.0	109.3	108.1	102.8	97.7	95.9
	ΔE	22.40	19.34	11.44	3.93	0.25	0.97	5.94	13.07	17.23	18.18
HF	S-Cl	1.9982	2.0019	2.0121	2.0226	2.0295	2.0312	2.0263	2.0174	2.0129	2.0119
	S-S	2.1365	2.1093	2.0499	2.0026	1.9811	1.9843	2.0149	2.0638	2.0906	2.0960
	S-S-Cl	106.8	106.5	105.8	105.6	106.1	106.0	104.2	100.7	97.6	96.4
	ΔE	18.44	15.75	9.27	3.06	0.12	1.04	5.04	9.48	11.74	12.19
MP2	S-Cl	1.9972	2.0029	2.0220	2.0414	2.0515	2.0535	2.0454	2.0244	2.0173	2.0159
	S-S	2.1571	2.1171	2.0305	1.9715	1.9469	1.9494	1.9817	2.0520	2.0917	2.0983
	S-S-Cl	105.0	105.0	105.1	105.9	107.4	107.6	105.7	100.8	96.5	95.0
	ΔE	20.22	17.32	10.16	3.34	0.14	1.18	6.09	11.97	14.86	15.42

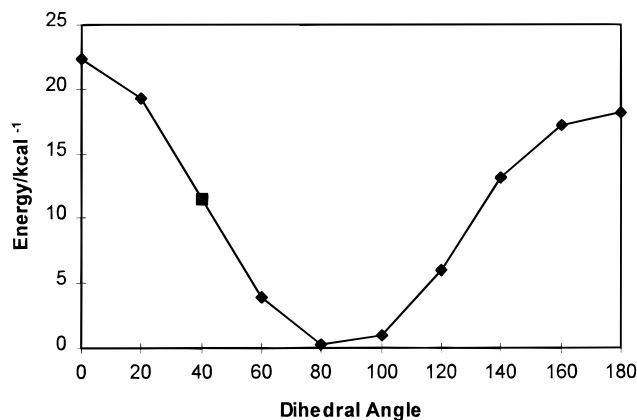


Figure 1. Change in energy with Cl-S-S-Cl dihedral at B3P86/6-311+G(3df).

TABLE 5: Expansion Coefficients (kcal mol⁻¹)

	V_1	V_2	V_3	V_4	V_5
HF	1.236	7.660	1.694	-0.165	0.207
MP2	0.388	8.953	1.728	-0.253	0.328
B3LYP	0.468	10.087	1.329	-0.164	0.344
B3P86	0.370	10.298	1.400	-0.122	0.372
B3PW91	0.443	10.308	1.384	-0.117	0.363

The three hybrid density functionals as well as ab initio methods predict the same trend in the change of S-S and S-Cl bond lengths with change of Cl-S-S-Cl torsion angle from 0° to 180°. The S-Cl bond length is shortest at $\tau = 0$ and becomes longer with increasing dihedral. The maximum is around $\tau = 100$. The S-S bond length is the maximum at the cis conformation and approaches the minimum at the equilibrium dihedral before increasing again. The predicted S-S-Cl angle is about 106° at $\tau = 0$ for the density functionals, rises to a maximum at nearly $\tau = 100$, and drops to its minimum value of ~96° at $\tau = 180$. The ab initio methods also show the same trend. Figure 1 shows the variation of relative energy as a function of the dihedral angle for the B3P86 functional.

As in the torsional potential of H₂S₂,³⁹ the potential energy function $V(\tau)$ can be expanded as a trigonometric series of the form,

$$V(\tau) = V_1 \cos \tau + V_2 \cos 2\tau + V_3 \cos 3\tau + V_4 \cos 4\tau + V_5 \cos 5\tau + \dots$$

where τ is the Cl-S-S-Cl dihedral angle. Fitting the calculated data of τ versus energy for the different methods, one obtains the different coefficients given in Table 5. The authors are not aware of any available experimental torsional potential function for comparison.

S₂Cl₂ → SSCI₂ Isomerization

The relative stabilities, as well as isomerization of S₂X₂ and SSX₂ (X = H, F, Cl) has, over the years, caused a lot of interest and still remains controversial. Experiment and theory have not been able to unequivocally resolve whether FSSF is more stable than SSF₂.^{43,44} Most of the experimental and highly correlated theoretical methods estimate the energy difference between FSSF and SSF₂ as ±3 kcal mol⁻¹. Recently, Schleyer and co-workers and Jursic independently determined the activation energy for the FSSF to SSF₂ isomerization using a variety of ab initio and density functional techniques.^{24,43}

The isomerization of ClSSCl to SSCI₂ has also caused considerable interest. Even though there is some evidence of

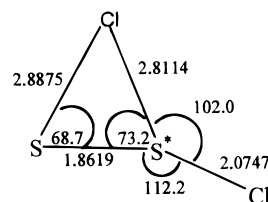


Figure 2. The transition state structure for the isomerization of S₂Cl₂ to SSCI₂ at B3LYP/6-311+G(3df).

TABLE 6: Geometry of SSCI₂

	S-S	S-Cl	S-S-Cl	Cl-S-Cl
HF/6-311+G(3df)	1.8887	2.0472	109.5	97.4
MP2/6-311+G(2df)	1.8721	2.1235	109.6	95.8
B3LYP6-311+G(3df)	1.8833	2.1529	110.0	97.4
B3P866-311+G(3df)	1.8743	2.1177	109.9	97.2
B3PW916-311+G(3df)	1.8765	2.1200	109.9	97.3
BLYP6-311+G(3df)	1.9023	2.2148	110.4	98.5
BP86/6-311+G(3df)	1.8926	2.1716	110.2	98.0
QCISD/6-311G(d)	1.9044	2.1674	110.0	97.0

the existence of SSCI₂, Steudel⁴⁵ in the low-temperature Raman spectra and Marsden²⁹ and co-workers in the microwave spectra of S₂Cl₂ failed to see any evidence of SSCI₂. While this by itself does not rule out the interconversion of S₂Cl₂ → SSCI₂, it indicates the activation energy for the isomerization might be higher than the 3 kcal mol⁻¹ barrier calculated by Soulouki and Bock⁴⁶ using CNDO/2.

The isomerization of ClSSCl to SSCI₂ has been investigated. The equilibrium structure of SSCI₂ at different theoretical levels have been given in Table 6. All theoretical models predict a further reduction in S-S bond distance. This is consistent with the reduction of S-S bond distance when FSSF gets transformed to SSF₂.²⁴ The density functionals do not predict much of a change in the S-S-Cl bond angle where as MP2 predicts a 2° increase in the S-S-Cl angle compared to S₂Cl₂.

The energies of transformation of S₂Cl₂ to SSCI₂ at HF, MP2, B3LYP, B3P86, and B3PW91 have been determined (Table 7). The theoretical models indicate that ClSSCl is more stable than SSCI₂ by 10–12.5 kcal mol⁻¹ at B3LYP, B3PW91, and B3P86 as well as at MP2. HF estimates ClSSCl to be almost twice as stable. Schleyer and co-workers²⁴ had estimated the relative stability to be around 29 kcal mol⁻¹ at HF/6-31G(d) basis. The addition of diffuse as well as d and f polarization functions in 6-311+G(3df) improves the accuracy of the prediction of HF as well as MP2 relative stabilities.

Assuming the isomerization is unimolecular and the 1,2 shift of the Cl atom proceeds via a three-membered ring transition state in which the migrating Cl is loosely bound to both S atoms (Figure 2), the energy of activation for the S₂Cl₂ to SSCI₂ transformation has been determined at HF, B3LYP, B3P86, and B3PW91 using the 6-311+G(3df) basis and at the 6-311+G(2df) basis for MP2. The density functionals predict a reduction in the S-S bond length in the transition state structure compared to both S₂Cl₂ and SSCI₂. MP2 predicts a longer S-S bond than either S₂Cl₂ or SSCI₂. The S-S-Cl bond angle and Cl-S-Cl bond angle predicted by MP2 and the density functionals are very different.⁴⁷

The activation energy of the isomerization is estimated to be between 40 and 43 kcal mol⁻¹ for the density functionals and about 48 kcal mol⁻¹ for MP2. HF estimates the activation barrier to be nearly 64 kcal mol⁻¹. As in the case of the isomerization of F₂S₂ to SSF₂, HF overestimates the barrier due to its lack of effective treatment of electron correlation. In contrast to the CNDO/2 barrier of Soulouki and Bock,⁴⁶ an activation barrier of around 40 kcal mol⁻¹ taken together with the relative stability

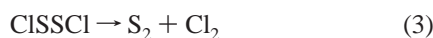
TABLE 7: Relative Energy (kcal mol⁻¹) and Activation Energy (kcal mol⁻¹) for S₂Cl₂ and SSCI₂^a

	<i>E</i> (S ₂ Cl ₂)	<i>E</i> (SSCl ₂)	<i>E</i> (TS)	Δ <i>E</i> ₁	Δ <i>E</i> ₂	Δ <i>E</i> ₃	<i>E</i> _{act1}	<i>E</i> _{act2}
HF/6-311+G(3df)	-1714.097667	-1714.060875	-1713.996453	23.09	21.40	50.26	63.51	40.43
MP2/6-311+G(2df)	-1714.801972	-1714.785569	-1714.725952	10.29	53.35	56.23	47.70	37.41
B3LYP/6-311+G(3df)	-1716.911699	-1716.892008	-1716.847236	12.36	46.43	56.26	40.45	28.09
B3P86/6-311+G(3df)	-1718.162683	-1718.142992	-1718.094237	12.36	51.69	61.82	42.95	30.59
B3PW91/6-311+G(3df)	-1716.702272	-1716.682299	-1716.633447	12.53	49.47	60.22	43.19	30.66
QCISD//6-311+G(3df) ^b	-1714.865302	-1714.840283		15.70	44.03	51.06		

^a *E*(S₂Cl₂), *E*(SSCl₂) and *E*(TS) are the absolute energies (in hartrees) of S₂Cl₂, SSCI₂, and their transition state, respectively. Δ*E*₁ is the relative unstability (kcal mol⁻¹) of SSCI₂ with respect to S₂Cl₂ (*E*(SSCl₂) - *E*(S₂Cl₂)). Δ*E*₂ and Δ*E*₃ are the energy changes associated with reactions 2 and 3, respectively. *E*_{act1} and *E*_{act2} are the activation energies (kcal mol⁻¹) with respect to S₂Cl₂ and SSCI₂, respectively. ^b Single point QCISD/6-311+G(3df) energy at QCISD/6-311G(d) geometry.

of CISSCl explains why SSCI₂ has not been detected spectroscopically along with the former.

Besides the unimolecular isomerization to SSCI₂, dichlorodisulfane can also decompose by the following two pathways:



The energetics for these two processes have been included in Table 7. The energy of transformation for the unimolecular isomerization is considerably lower than the above two processes at hybrid density functional as well as MP2 and QCISD levels. Since the activation energy for the isomerization (*E*_{act1}) at these correlated levels is lower than the energy of transformation (Δ*E*₂ or Δ*E*₃) by either reaction 2 or 3, the isomerization to SSCI₂ is the more favorable than the other two pathways shown above. However, the prediction at the HF level is ambiguous. HF estimates a lower energy of transformation to CISS[•] + Cl[•] than to SSCI₂.⁴⁸ This could be due to the lack of effective treatment of electron correlation in HF.

Conclusion

The density functionals, particularly B3P86 and B3PW91, reproduce the experimental S-S and S-Cl bond lengths to the same level of accuracy as MP2. This makes it an attractive alternative compared to traditional ab initio methods. Use of diffuse and d and f polarization functions is essential to get more accurate bond lengths even though it has little effect on bond angles. The inclusion of diffuse and 3df functions reduces the RMS deviation of predicted frequencies by half. MP2 produces the lowest RMS deviation in frequency at 6-311G(d). The density functionals and MP2 predict comparable cis and trans barrier to rotation. The isomerization of S₂Cl₂ to SSCI₂ is not seen in low-temperature spectra because of a barrier higher than 40 kcal mol⁻¹. This is the more likely reaction pathway, as determined by the correlated methods, compared to the other two possible decomposition pathways. The result obtained by the HF method are ambiguous however as it shows a lower energy of transformation to radical decomposition.

Acknowledgment. We thank Prof. Peter Politzer and his research group for computer time for part of the work. The suggestions of the anonymous reviewers, which made this manuscript more complete, are greatly appreciated.

References and Notes

- (1) Lister, D. G.; Macdonald, J. N.; Owen, N. L. *Internal Rotation and Inversion*; Academic Press: London, 1978.
- (2) Jug, K.; Iffert, R. *J. Mol. Struct. (THEOCHEM)* **1989**, *186*, 347. Hinchliffe, A. *J. Mol. Struct.* **1979**, *55*, 127. Krüger, H.; Preuss, Z. *Z. Naturforsch A* **1983**, *38*, 463.

(3) Parr, R. G.; Yang, W. *Density-Functional Theory of Atoms and Molecules*; Oxford University: New York, 1989.

(4) Seminario, J. M.; Politzer, P., Eds. *Modern Density Functional Theory A Tool for Chemistry*; Elsevier: Amsterdam, 1995.

(5) Hehre, W. J.; Radom, L.; Schleyer, P. von R.; Pople, J. A. *Ab Initio Molecular Orbital Theory*; Wiley: New York, 1986.

(6) Frisch, M. J.; Trucks, G. W.; Schlegel, H. B.; Gill, P. M. W.; Johnson, B. G.; Robb, M. A.; Cheeseman, J. R.; Keith, T.; Petersson, G. A.; Montgomery, J. A.; Raghavachari, K.; Al-Laham, M. A.; Zakrzewski, V. G.; Ortiz, J. V.; Foresman, J. B.; Cioslowski, J.; Stefanov, B. B.; Nanayakkara, A.; Challacombe, M.; Peng, C. Y.; Ayala, P. Y.; Chen, W.; Wong, M. W.; Andres, J. L.; Replogle, E. S.; Gomperts, R.; Martin, R. L.; Fox, D. J.; Binkley, J. S.; Defrees, D. J.; Baker, J.; Stewart, J. P.; Head-Gordon, M.; Gonzalez, C.; Pople, J. A. *Gaussian 94*, revision D.4; Gaussian, Inc.: Pittsburgh, PA, 1995.

(7) Murtagh, B. A.; Sargent, R. W. H. *Comput. J.* **1970**, *13*, 185.

(8) Møller, C.; Plesset, M. S. *Phys. Rev.* **1934**, *46*, 618.

(9) Pople, J. A.; Head-Gordon, M.; Raghavachari, K. *J. Chem. Phys.* **1987**, *87*, 5968.

(10) Becke, A. D. *Int. J. Quantum Chem.* **1994**, *S28*, 625.

(11) Becke, A. D. *J. Chem. Phys.* **1993**, *98*, 5648.

(12) Lee, C.; Yang, W.; Parr, R. G. *Phys. Rev. B* **1988**, *37*, 785.

(13) Perdew, J. P. *Phys. Rev. B* **1986**, *33*, 8822.

(14) Perdew, J. P. *Phys. Rev. B* **1987**, *34*, 7046.

(15) Perdew, J. P.; Wang, Y. *Phys. Rev.* **1992**, *B45*, 13244.

(16) Hohenberg, P.; Kohn, W. *Phys. Rev.* **1964**, *136*, B864. Kohn, W.; Sham, L. *Phys. Rev.* **1965**, *140*, A1133. Slater, J. C. *Quantum Theory of Molecular and Solids*; McGraw-Hill: New York, 1974; Vol. 4.

(17) Vosko, S. H.; Wilk, L.; Nusair, M. *Can. J. Phys.* **1980**, *58*, 1200.

(18) Becke, A. D. *Phys. Rev. A* **1988**, *38*, 3098.

(19) Frisch, M. J.; Pople, M. J.; Binkley, J. S. *J. Chem. Phys.* **1984**, *80*, 3265. Clark, T.; Chandrasekhar, J.; Spitznagel, G. W.; Schleyer, P. v. R. *J. Comput. Chem.* **1983**, *4*, 294.

(20) Peng, C.; Schlegel, H. B. *Israel J. Chem.* **1993**, *33*, 449.

(21) Cárdenas-Jirón, G. I.; Cárdenas-Lailhacar, C.; Toro-Labbé, A. *J. Mol. Struct. (THEOCHEM)* **1993**, *282*, 113.

(22) Hirota, E. *Bull. Chem. Soc. Jpn.* **1958**, *31*, 130.

(23) Samdal, S.; Mastryukov V. S.; Boggs, J. E. *J. Mol. Struct. (THEOCHEM)* **1994**, *309*, 21.

(24) Bickelhaupt, F. M.; Solà, M.; Schleyer, P. v. R. *J. Comput. Chem.* **1995**, *16* (4), 465.

(25) Altmann, J. A.; Handy, N. C.; Ingamells, V. E. *Int. J. Quantum Chem.* **1996**, *57*, 533.

(26) Dirac, P. A. M. *Camb. Philos. Soc.* **1930**, *26*, 376.

(27) Altmann, J. A.; Handy, N. C.; Ingamells, V. E. *Mol. Phys.* **1997**, *92* (3), 339.

(28) Woon, D. E.; Dunning, T. H. *J. Chem. Phys.* **1993**, *98*, 1358.

(29) Marsden, C. J.; Brown, R. D.; P. D. Godfrey, *J. Chem. Soc., Chem. Comm.* **1979**, 399.

(30) Beagley, B.; Eckersely, G. H.; Brown, D. P.; Tomlinson, D. *Trans. Faraday Soc.* **1969**, *65*, 2300.

(31) Caron, A.; Donohue, J. *Acta Cryst.* **1965**, *18*, 562.

(32) The energy difference between 6-311+G(3df) and 6-31G(d) basis for HF, LSDA, B3LYP, BLYP, BP86, B3P86, and B3PW91 is about 0.15 hartrees. The energy difference for MP2 and QCISD is about 0.36 hartrees.

(33) The 6-311+G(3df) energies for LSDA, HF, MP2, QCISD, B3PW91, BLYP, B3LYP, BP86, and B3P86 are -1712.541429, -1714.097667, -1714.812739, -1714.865302, -1716.702272, -1716.862122, -1716.911699, -1717.035363, and -1718.162683, respectively.

(34) Wong, M. W. *Chem. Phys. Lett.* **1996**, *256*, 391.

(35) Frankiss, S. G. *J. Mol. Struct.* **1968**, *2* (4), 271.

(36) Das, D. Ph.D. Thesis, University of New Orleans, LA, 1999.

(37) Winniewisser, G.; Winniewisser, M.; Gordy, W. *J. Chem. Phys.* **1968**, *3465*. Surjan, P. R.; Mayer, I.; Kertész, M. *J. Chem. Phys.* **1982**, *77*, 2454.

(38) The MP2/6-311+G(3df) dipole moments for H₂S₂, S₂F₂, and dimethyl ether (DME) are 1.25, 1.74, and 1.48 D respectively. The HF/6-311+G(3df) dipole moments for H₂S₂, S₂F₂, DME, and dimethyl sulfide are 1.26, 1.31, 1.37, and 1.76, respectively.

(39) Koput, J. *Chem. Phys. Lett.* **1996**, 259, 146.

(40) Mastryukov, V. S.; Boggs, J. E.; Samdal, S. *J. Mol. Struct. (THEOCHEM)* **1993**, 288, 225.

(41) The BLYP, BP86, and LSDA cis barriers at 6-311+G(3df) basis are 24.25, 24.62, and 24.78 kcal mol⁻¹, respectively.

(42) The trans barriers at 6-311+G(3df) basis for BLYP, BP86, and LSDA are 20.69, 20.99, and 21.37 kcal mol⁻¹ respectively.

(43) Jursic, B. S. *J. Comput. Chem.* **1996**, 17 (7), 835.

(44) See ref 24 and references therein.

(45) Steudel, R.; Jensen, D.; Plinke, B. *Z. Naturforsch* **1987**, 42b, 163.

(46) Solouki, B.; Bock, H. *Inorg. Chem.* **1977**, 16, 665.

(47) The S-S, S-S-Cl, and Cl-S-Cl geometrical parameters of the transition state at MP2/6-311+G(2df) basis are 1.9755 Å, 65.2°, and 130.3°, respectively.

(48) The lower energy of transformation for the radical decomposition is also predicted at other basis sets for HF calculations. So this is not a basis set artifact.